

Multisystem FDG-avid lesions mimicking malignancy in a teenager with hyper-IgE syndrome: A case study with literature review

Fatemeh Saboktakin, Saeed Farzanefar, Nasim Vahidfar, Shaghayegh Ranjbar, Niloofar Tabatabaeian*

Department of Nuclear Medicine, Vali-Asr Hospital, Tehran University of Medical Sciences, Tehran, Iran

ARTICLE INFO

Article type:

Case Report

Article history:

Received: 24 Sep 2025

Revised: 16 Feb 2026

Accepted: 21 Feb 2026

Keywords:

Hyper-IgE syndrome

Job's syndrome

FDG-PET

ABSTRACT

Hyper-IgE Syndrome (HIES) is a rare immunodeficiency predisposing patients to infections, inflammation, and occasional neoplasia. We report a 17-year-old boy with HIES who presented with severe right thigh pain. FDG-PET/CT demonstrated a right adrenal mass ($SUV_{max}=5.4$), multiple pulmonary nodules, and a lytic-sclerotic femoral lesion ($SUV_{max}=4.6$), initially suggesting disseminated malignancy. Biopsy confirmed acute osteomyelitis and a benign spindle cell tumor of the adrenal gland. Two months later, persistent fever and elevated ESR prompted re-evaluation, revealing intense FDG uptake in the thoracic aorta ($SUV_{max}=20.5$) consistent with large vessel vasculitis, later confirmed by angiography. The combination of infection, benign tumor, and vasculitis illustrates the broad FDG uptake spectrum in HIES and the risk of misdiagnosis as malignancy. Integration of clinical, imaging, and histopathologic data was critical for accurate diagnosis. This case highlights FDG-PET/CT's value in detecting inflammatory vascular disease and monitoring therapy, while reinforcing the importance of biopsy for definitive diagnosis. In immunodeficient patients, a multimodal diagnostic approach is essential to distinguish between malignant and benign FDG-avid lesions.

► Please cite this paper as:

Saboktakin F, Farzanefar S, Vahidfar N, Ranjbar Sh, Tabatabaeian N. Multisystem FDG-avid lesions mimicking malignancy in a teenager with hyper-IgE syndrome: A case study with literature review. *Asia Ocean J Nucl Med Biol.* 2026; 14(2): 219-223. doi: 10.22038/aojnmb.2026.91014.1671

Introduction

Hyper-IgE Syndrome (HIES), or Job's Syndrome, is a rare immunodeficiency characterized by high serum IgE, eosinophilia, eczema, and recurrent staphylococcal infections (1). It is commonly associated with STAT3 mutations and has systemic manifestations including pulmonary infections, skeletal abnormalities, and vasculopathies (2). Due to dysregulated immunity, HIES patients may develop atypical inflammatory lesions that mimic malignancy on functional imaging such as ^{18}F -FDG PET/CT (3). This poses a diagnostic dilemma, as FDG uptake is not specific to neoplasia but may reflect infection, inflammation, or immune activation (4).

Case Presentation

A 17-year-old boy with known hyper-IgE syndrome (HIES) presented with right thigh pain, fever, and fatigue. His history included recurrent bacterial infections and atopic dermatitis.

Initial FDG-PET/CT (figure 1) findings included:

- FDG-avid right adrenal mass (51×55 mm, $SUV_{max}=5.4$)
- Small mildly FDG-avid left adrenal nodule
- Multiple FDG-avid pulmonary nodules
- Lytic-sclerotic lesion in the right femur with periosteal reaction ($SUV_{max}=4.6$), suspicious for malignant bone lesion (more in favor of Ewing sarcoma).

* Corresponding author: Niloofar Tabatabaeian. Department of Nuclear Medicine, Vali-Asr Hospital, Tehran University of Medical Sciences, Tehran 1419733141, Iran. Tel: +989916457646; Email: Niloofartabatabaeian97@gmail.com

© 2026 *mums.ac.ir* All rights reserved.

This is an Open Access article distributed under the terms of the Creative Commons Attribution License (<http://creativecommons.org/licenses/by/3.0>), which permits unrestricted use, distribution, and reproduction in any medium, provided the original work is properly cited.

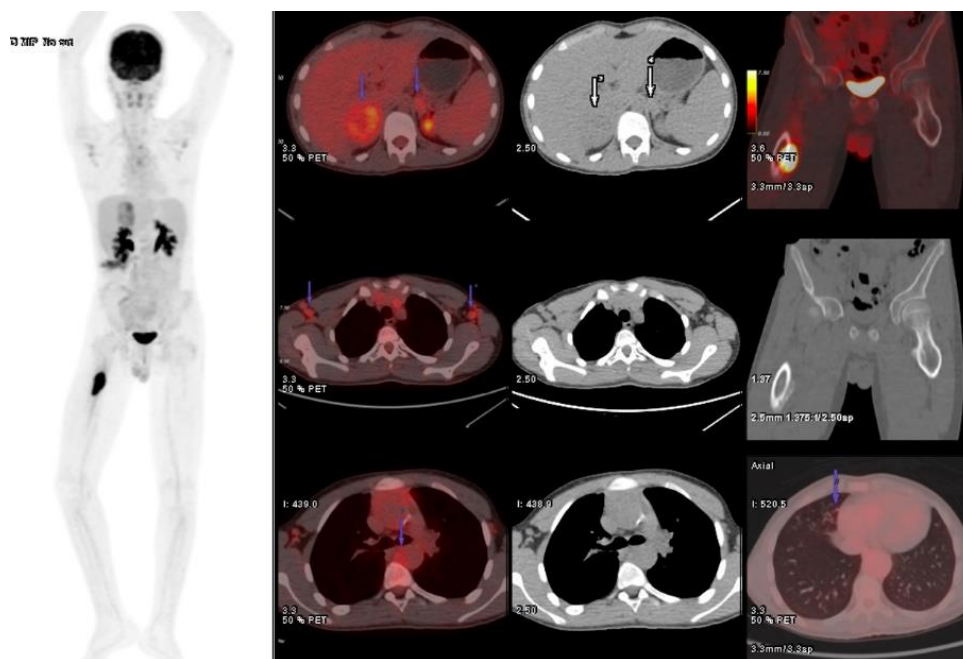


Figure 1. 17 y/o patient with history of HIES underwent PET/CT scan due to right femoral pain. The study is suggestive of FDG avid right adrenal mass (measuring 51×55mm, $SUV_{max}=5.4$), mildly FDG avid left adrenal nodule (measuring 18×12mm, $SUV_{max}=2.7$) and few pulmonary nodules with mild FDG uptake, largest one located in RML (measuring 6mm, $SUV_{max}=1.4$), hypermetabolic lytic sclerotic right femoral osseous lesion along with periosteal reaction ($SUV_{max}=4.6$) and multiple hypermetabolic bilateral axillary lymph nodes, some with thick cortex (measuring up to 12×12mm, SUV_{max} up to 2.9)

These findings suggested a malignant bone tumor with possible adrenal and pulmonary metastases. Biopsies were performed on the right femur and adrenal mass.

Histopathology results:

- Right femur: Acute osteomyelitis with dense neutrophilic infiltration, edema, vascular congestion, and early osteocyte necrosis.
- Right adrenal mass: Leiomyoma composed of spindle cells with uniform nuclei, eosinophilic cytoplasm, no mitotic activity, and chronic inflammatory infiltrates in hyalinized and edematous stroma. IHC showed h-caldesmon and desmin positivity (smooth muscle origin), with negative ALK, SOX10, Myogenin, and MyoD1. Ki-67 index was ~3-4%.

The patient improved with antibiotic therapy for osteomyelitis. However, two months later, persistent fever, elevated ESR, and echocardiographic

findings (LVEF=50-55%, turbulent flow) raised suspicion for vasculitis.

Follow-up PET/CT (Figure 2) findings:

- Semi-circumferential intense FDG uptake ($SUV_{max}=20.5$) in the anterior descending thoracic aorta (10 to 1 o'clock below the carina)
- Circumferential intermediate-grade uptake ($SUV_{max}=2.3$) along the remaining thoracic aorta-grade 2 compared to liver-suggestive of large vessel vasculitis
- Previously FDG-avid right femoral lesion now appeared as non-avid cortical thickening of the midshaft femoral diaphysis, consistent with chronic or treated osteomyelitis

Angiography confirmed post-subclavian coarctation and diffuse aortic wall thickening, consistent with large vessel vasculitis.

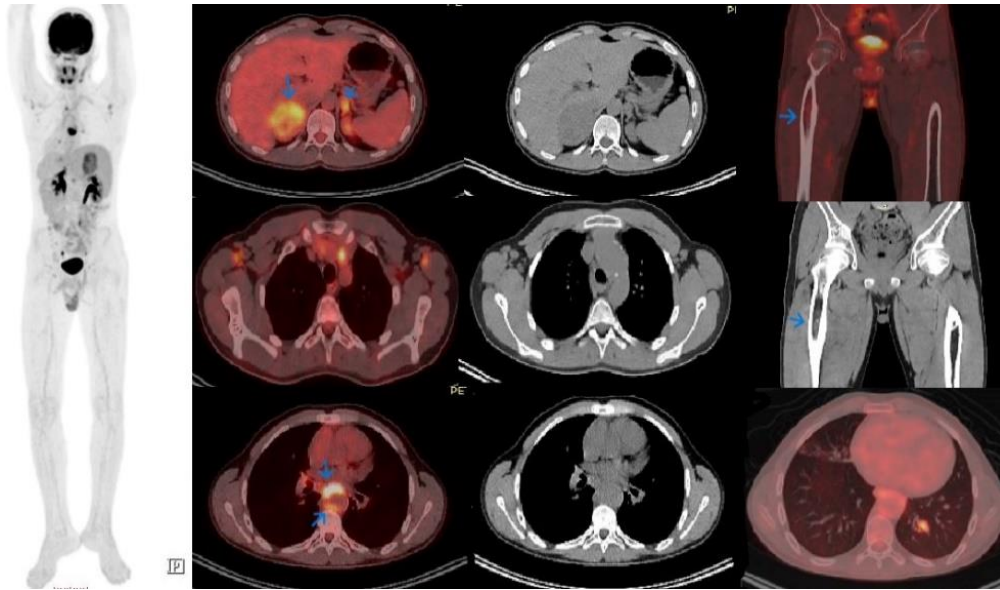


Figure 2. PET/CT Follow-up scan reveals FDG avid right adrenal mass (measuring 40×42mm, $SUV_{max}=5.2$) and mildly FDG avid left adrenal nodule which are stable since previous PET study. Previously noted pulmonary nodule in RML resolved in current study and a new pulmonary nodule appears in the LLL (measuring 13mm, $SUV_{max}=4$). Interval developed semi-circumferential intense FDG uptake ($SUV_{max}=20.5$) is seen in the anterior descending thoracic aorta (10 to 1 o'clock below the carina), circumferential intermediate-grade uptake ($SUV_{max}=2.3$) along the remaining thoracic aorta is also noted. Previously noted hypermetabolic axilla lymph nodes are again noted which are stable since previous study. Also, previously noted FDG-avid right femoral lesion now appeared as non-FDG-avid cortical thickening in the midshaft of femoral diaphysis, consistent with chronic or treated osteomyelitis

Discussion

This case illustrates the diagnostic challenges of interpreting FDG-PET/CT in primary immunodeficiency syndromes such as hyper-IgE syndrome (HIES), where increased FDG uptake may reflect malignancy, infection, inflammation, or benign tumors (5,6). In this patient, the initial FDG-PET/CT revealed a suspicious bone lesion and adrenal mass. Due to persistent fever and elevated ESR, a follow-up scan identified large vessel vasculitis. Final diagnoses included acute osteomyelitis, adrenal leiomyoma, and Takayasu-like vasculitis-confirmed via echocardiography, angiography, and histopathology.

Histology of the adrenal mass showed a benign spindle cell tumor with no mitotic activity, embedded in hyalinized and edematous stroma with chronic inflammation. IHC confirmed smooth muscle origin (positive for h-caldesmon, desmin) and excluded IMT (ALK-), schwannoma (SOX10-), and rhabdomyosarcoma (Myogenin-, MyoD1-). A low Ki-67 index (3-4%) supported the diagnosis of leiomyoma, a rare adrenal tumor likely from vascular smooth muscle (7-9). The bone lesion, initially suggestive of malignancy (e.g., Ewing sarcoma), was confirmed as acute osteomyelitis, consistent with HIES-related infection susceptibility (10).

Vasculitis was suspected due to persistent

fever, elevated ESR, and echocardiographic signs of turbulent flow (LVEF=50-55%).

PET/CT showed focal increased FDG uptake in the thoracic aorta ($SUV_{max}=20.5$ anteriorly, 2.3 elsewhere), suggestive of vasculitis (11). Angiography revealed post-subclavian coarctation and diffuse aortic thickening, confirming the diagnosis (12).

HIES, often caused by STAT3 mutations, and predisposes to infections, connective tissue anomalies, and rare vasculitis (13). Freeman et al. emphasized the role of dysregulated cytokines in osteomyelitis, vasculitis, and chronic inflammation in benign tumors (3). This triad of lesions reflects immune dysregulation and complicates FDG interpretation.

Although highly sensitive, FDG-PET/CT lacks specificity in immunocompromised hosts, where infection, inflammation, and benign lesions may mimic cancer (4). Sathegke et al. reported 85-90% sensitivity but only 50% specificity in such settings (14). The adrenal leiomyoma's diagnosis was supported by IHC markers distinguishing it from sarcomas (15, 16). Similarly, Ewing sarcoma and osteomyelitis, with overlapping imaging features, require biopsy for differentiation (17).

PET/CT also proved valuable in assessing vasculitis, with Sađer et al. documenting high FDG uptake in Takayasu arteritis, resolving after treatment (18). Marco et al. advocated

combining PET/CT and CT angiography to assess inflammation and vascular morphology simultaneously (19). Thus, integrating imaging, clinical, and pathological data was essential for accurate diagnosis and management in this complex HIES case.

Conclusion

In conclusion, this case highlights the complexity of interpreting FDG-PET/CT in HIES and similar conditions. The literature underscores the importance of recognizing benign mimics of malignancy, such as spindle cell tumors, and rare complications like vasculitis in HIES. Histological confirmation is critical, as metabolically active lesions in HIES may represent benign or inflammatory processes rather than malignancy. Also, clinicians must employ a multimodal diagnostic strategy to avoid misdiagnosis and guide appropriate management.

Acknowledgement

The authors would like to acknowledge the support and contributions that made this work possible. The authors received no financial support for this study and have no conflicts of interest to disclose.

Conflict of interest

None to declare.

Ethical consideration

Written informed consent was obtained from the patient for publication of this case report.

Contribution of author

Drafting of manuscript: Shaghayegh Ranjbar. Data analysis: Fatemeh Saboktakin, Saeed Farzanefar, Nasim Vahidfar. Manuscript revision: Niloofar Tabatabaeian, Fatemeh Saboktakin.

References

- Grimbacher B, Holland SM, Puck JM. Hyper-IgE syndromes. *Immunological reviews*. 2005; 203(1): 244-50.
- Minegishi Y, Saito M, Tsuchiya S, Tsuge I, Takada H, Hara T, et al. Dominant-negative mutations in the DNA-binding domain of STAT3 cause hyper-IgE syndrome. *Nature*. 2007; 448(7157): 1058-62.
- Freeman AF, Holland SM. Clinical manifestations, etiology, and pathogenesis of the hyper-IgE syndromes. *Pediatric Research*. 2009; 65(7): 32-7.
- Love C, Tomas MB, Tronco GG, Palestro CJ. FDG PET of infection and inflammation. *Radiographics*. 2005; 25(5): 1357-68.
- Zhuang H, Jian QY, Alavi A. Applications of fluorodeoxyglucose-PET imaging in the detection of infection and inflammation and other benign disorders. *Radiologic Clinics*. 2005; 43(1):121-34.
- Noriega-Álvarez E, Gadea LD, Diez MO, Valgañón VP, Viedma SS, Jiménez RG. Role of Nuclear Medicine in the diagnosis of musculoskeletal infection: A review. *Revista Española de Medicina Nuclear e Imagen Molecular (English Edition)*. 2019; 38(6): 397-407.
- Sakellariou M, Dellaportas D, Peppas M, Schizas D, Pikoulis E, Nastos K. Review of the literature on leiomyoma and leiomyosarcoma of the adrenal gland: a systematic analysis of case reports. *In vivo*. 2020; 34(5): 2233-48.
- Coffin CM, Hornick JL, Fletcher CD. Inflammatory myofibroblastic tumor: comparison of clinicopathologic, histologic, and immunohistochemical features including ALK expression in atypical and aggressive cases. *The American journal of surgical pathology*. 2007; 31(4): 509-20.
- Ducatman BS, Scheithauer BW, Piepgras DG, Reiman HM, Ilstrup DM. Malignant peripheral nerve sheath tumors. A clinicopathologic study of 120 cases. *Cancer*. 1986; 57(10): 2006-21.
- Lew DP, Waldvogel FA. Osteomyelitis. *The Lancet*. 2004; 364(9431):3 69-79.
- Zhuang H, Alavi A. 18-Fluorodeoxyglucose positron emission tomographic imaging in the detection and monitoring of infection and inflammation. *In Seminars in Nuclear Medicine* 2002; 32(1): 47-59.
- Keser G, Aksu K, Direskeneli H. Takayasu arteritis: an update. *Turkish Journal of Medical Sciences*. . 2018; 48(4): 681-697.
- Holland SM, DeLeo FR, Elloumi HZ, Hsu AP, Uzel G, Brodsky N, et al. STAT3 mutations in the hyper-IgE syndrome. *New England Journal of Medicine*. 2007; 357(16): 1608-19.
- Sathekge M, Maes A, Van de Wiele C. FDG-PET imaging in HIV infection and tuberculosis. *In Seminars in nuclear medicine* 2013; 43(5):349-366.
- Watanabe K, Tajino T, Sekiguchi M, Suzuki T. h-Caldesmon as a specific marker for smooth muscle tumors: comparison with other smooth muscle markers in bone tumors. *American journal of clinical pathology*. 2000; 113(5): 663-8.
- Kumar R, Xiu Y, Yu JQ, Takalkar A, El-Haddad G, Potenta S, et al. ¹⁸F-FDG PET in evaluation of adrenal lesions in patients with lung cancer. *Journal of Nuclear Medicine*. 2004;

- 45(12): 2058-62.
17. Durbin M, Randall RL, James M, Sudilovsky D, Zoger S. Ewing's sarcoma masquerading as osteomyelitis. *Clinical Orthopaedics and Related Research*. 1998; 357: 176-85.
 18. Sağer S, Yılmaz S, Özhan M, Halaç M, Ergül N, Çiftçi H, et al. F-18 Fdg PET/CT findings of a patient with Takayasu arteritis before and after therapy. *Molecular Imaging and Radionuclide Therapy*. 2012; 21(1): 32.
 19. Marco DN, Gilabert R, Cid MC, Muxí A, Prieto-González S. Hybrid ¹⁸F-FDG-PET with CT angiography for diagnosis of Takayasu arteritis. *Rheumatology (Oxford)*. 2024; 63(8): e217–e218.